

# Current noise of a single-electron transistor coupled to a nanomechanical resonator

A. D. Armour

*School of Physics and Astronomy, University of Nottingham, Nottingham NG7 2RD, United Kingdom*

(Dated: October 24, 2018)

The current noise spectrum of a single-electron transistor (SET) coupled to a nanomechanical resonator is calculated in the classical regime. Correlations between the charge on the SET island and the position of the resonator give rise to a distinctive noise spectrum which can be very different from that of the uncoupled SET. The current noise spectrum of the coupled system contains peaks at both the frequency of the resonator and double the resonator frequency, as well as a strong enhancement of the noise at low frequencies. The heights of the peaks are controlled by the strength of the coupling between the SET and the resonator, the damping of the resonator, and the temperature of the system.

## I. INTRODUCTION

Nanoelectromechanical systems in which a nanomechanical resonator is coupled to a mesoscopic conductor, such as a single-electron transistor (SET), form a new class of mesoscopic system in which there is a fascinating interplay between the electrical and mechanical degrees of freedom. Coupling to nanomechanical degrees of freedom can modify the transport properties of mesoscopic conductors substantially, giving rise to a number of novel phenomena such as electron shuttling<sup>1,2</sup> and phonon blockade effects.<sup>3,4</sup> Furthermore, nanoelectromechanical systems have important potential applications as ultra-sensitive force detectors.<sup>5</sup>

A nanomechanical resonator coated with a thin metal layer can be coupled to a SET as a mechanically compliant voltage-gate.<sup>6,7</sup> Under such circumstances the tunnelling rates of electrons through the SET island, and hence the current flowing, depend sensitively on the position of the resonator.<sup>6,7,8,9</sup> It has been suggested that the SET could act as a quantum-limited displacement detector for micron-sized resonators<sup>6,7,10</sup> thus making it potentially very important both for read-out of the resonator's motion in force sensing applications<sup>11</sup> and for exploring quantum effects in electromechanical systems.<sup>12,13</sup> However, fluctuations in the charge on the SET island exert a stochastic force back on the resonator, affecting its motion, and hence also the average current through the SET.<sup>10,14</sup> Furthermore, the coupling between the resonator and the SET also has an important influence on the SET current noise.

The effect on the dynamics of a nanomechanical resonator of coupling to a mesoscopic conductor has been investigated by a number of authors.<sup>1,2,14,15,16,17,18</sup> For systems where the nanomechanical resonator forms a compliant voltage gate adjacent to either a SET<sup>14,17</sup> or a quantum point contact,<sup>15</sup> it has been found that the interaction with the electrons drives the resonator into a steady-state very similar to a thermal state, with an effective temperature and damping constant. In particular, when the resonator is treated as a quantum system it is found that whenever the energy associated with the bias voltage applied across the conductor is much greater than the energy quanta of the resonator, the electrons rapidly dephase the resonator and heat it to an effective temperature proportional to the bias voltage.<sup>15,16,17</sup> An analysis of the dynamics of a resonator coupled to a SET where the resonator is treated as a classical system leads to very similar conclusions in the regime where the applied bias voltage is relatively large and the charge dynamics of the SET is adequately described by the orthodox model.<sup>14</sup>

Although the dynamics of a nanomechanical resonator coupled to a mesoscopic conductor has been investigated for a number of different systems and regimes, there has been little systematic study of the concomitant current-noise spectrum of the mesoscopic conductor. Knowledge of the current-noise spectrum in nanoelectromechanical systems is of interest both because it sets limits on the sensitivity with which the current can be used as measure of the motion of the resonator and, more generally, because it has long been recognized that the current noise of mesoscopic conductors provides important additional information, beyond that available from simple average-current properties, about the interactions which the conduction electrons undergo.<sup>19</sup> In this paper the current noise of a SET coupled to a nanomechanical resonator is calculated in the classical regime using an extension of the master equation approach developed in Ref. 14. It is found that the current noise spectrum of the SET-resonator system can be very different from that of the uncoupled SET. In particular, the interactions between the resonator and the transport electrons can strongly enhance the SET current noise at low frequencies and give rise to additional peaks in the noise spectrum at the resonator frequency and at twice that value.

This paper is organized as follows. In Sec. II the dynamical model of the coupled resonator-SET system that forms the basis of the following calculations is introduced. Then in Sec. III, the relationship between the overall current noise spectrum of the SET and the spectrum of the charge noise on the island and the noise spectra of the tunnel currents between the island and the leads is described. In Secs. IV and V the noise spectra of the tunnel currents through the SET junctions and the charge noise on the SET island are obtained, respectively. The full current noise

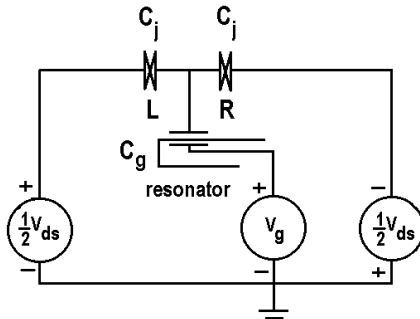


FIG. 1: Circuit diagram for the coupled SET-resonator system. The SET island lies between the two tunnel junctions which are assumed to have the same capacitance  $C_j$ . Under the drain-source voltage shown,  $V_{ds}$ , the electrons tend to flow through the SET island from right to left. The resonator is situated adjacent to the SET island and acts as a gate capacitor.

spectrum of the coupled SET-resonator system is obtained in Sec. VI. Finally, Sec. VII contains the conclusions.

## II. MODEL OF THE COUPLED SET-RESONATOR SYSTEM

A schematic diagram of the SET-resonator system is shown in Fig. 1. For simplicity, we have assumed a symmetric arrangement of capacitances and voltages. The SET island is connected to current leads by tunnel junctions with capacitance  $C_j$  and resistance  $R$ . The total voltage applied across the SET island is  $V_{ds}$ . The nanomechanical resonator forms the gate capacitor, with a capacitance  $C_g(x)$ , and a voltage  $V_g$  applied to it. The gate capacitance depends on the displacement of the resonator,  $x$ , about its equilibrium separation from the SET island,  $d$ . The resonator is displaced from its equilibrium position by fluctuations in the SET charge and by thermal fluctuations of the resonator itself, but for realistic systems<sup>6,7,14</sup> the resulting motion is on a scale much less than the equilibrium separation (i.e.  $x \ll d$ ), hence an expansion of the capacitance to linear order is sufficient and we may write  $C_g(x) = C_g(1 - x/d)$ , where  $C_g$  is a constant.<sup>9,10,14</sup> The gate capacitance is also assumed to be much less than that of the junction capacitances,  $C_g \ll C_j$ , which reflects the situation in typical devices.

Under a relatively wide range of conditions, the coupled dynamics of a nanomechanical resonator and a SET can be described using a master equation formalism.<sup>14</sup> Within this formalism, the SET is assumed to be within the regime where the orthodox model is valid and the resonator is treated as a classical harmonic oscillator, with angular frequency  $\omega_0$ , and effective mass  $m$ . The effects of damping processes on the resonator, beyond those due to interactions with the SET, can be taken into account by including an extrinsic damping rate,  $\gamma_e$ . The orthodox model describes electron transport through the SET away from the Coulomb blockade regions so that processes other than sequential tunnelling of electrons may be neglected.<sup>20</sup> The nanomechanical resonator is expected to behave classically whenever the bias voltage applied to the SET is much greater than the energy quanta of the resonator, i.e.  $eV_{ds} \gg \hbar\omega_0$ .<sup>15</sup> Complete details of the derivation, justification and analysis of this classical model for the coupled SET-resonator system are given in Ref. 14.

When the background temperature of the SET-resonator system,  $T_e$ , is much less than the charging energy of the SET island,  $e^2/2C_j \gg k_B T_e$ , and the bias voltage is not too large, the charge state of the SET island can be assumed to be limited to two possible values,  $N$  and  $N + 1$  excess electrons, and a pair of coupled master equations can be derived for the SET-resonator system. The bias voltage is also assumed to be much greater than the background temperature,  $eV_{ds} \gg k_B T_e$ , and so the effects of thermal fluctuations on the electron tunnel rates are neglected.<sup>14,20</sup> Writing  $P_{N(N+1)}(x, u; t)$  as the probability of having  $N(N + 1)$  electrons on the SET island and finding the resonator at position  $x$  and with velocity  $u$ , the master equations for the evolution of the probability distributions take the form<sup>14</sup>

$$\frac{\partial P_N}{\partial t} = \omega_0^2 x \frac{\partial P_N}{\partial u} - u \frac{\partial P_N}{\partial x} + \frac{\partial}{\partial u} \left( \gamma_e u P_N + \frac{G}{2m^2} \frac{\partial P_N}{\partial u} \right) + \left( \Gamma_L P_{N+1} - \Gamma_R P_N - \frac{m\omega_0^2 x_0}{Re^2} x P \right) \quad (1)$$

$$\frac{\partial P_{N+1}}{\partial t} = \omega_0^2 (x - x_0) \frac{\partial P_{N+1}}{\partial u} - u \frac{\partial P_{N+1}}{\partial x} + \frac{\partial}{\partial u} \left( \gamma_e u P_{N+1} + \frac{G}{2m^2} \frac{\partial P_{N+1}}{\partial u} \right) - \left( \Gamma_L P_{N+1} - \Gamma_R P_N - \frac{m\omega_0^2 x_0}{Re^2} x P \right) \quad (2)$$

where  $P(x, u; t) = P_N(x, u; t) + P_{N+1}(x, u; t)$ ,  $G = 2mk_B T_e \gamma_e$  and  $\Gamma_{L(R)}$  is the position-independent part of the tunnel rate through the  $L(R)$  junction. The length-scale  $x_0$  has a simple interpretation: it is the amount by which the equilibrium separation between the SET and the resonator changes when the charge on the SET island changes from  $N$  to  $N + 1$ .

The master equations [Eqs. (1) and (2)] assume that the bias voltage applied across the system is the dominant energy-scale and the probability distributions for the resonator are strongly peaked at  $x \sim x_0$ . Under such circumstances, which are readily met in practicable resonator-SET systems,<sup>14</sup> tunnelling processes that go against the direction imposed by the bias voltage may be neglected. The resulting master equations can be used to extract equations of motion for the average properties of the resonator and SET, and to characterize the steady-state of the system. Furthermore, the master equations provide the necessary information about the coupled dynamics of the SET-resonator system to allow the derivation of the SET current noise spectrum.

Analysis of the coupled master equations<sup>14</sup> shows that the SET electrons act on the resonator like another thermal bath (in addition to the substrate to which the resonator is attached) which can be characterized by an intrinsic temperature,  $T_i$ , proportional to  $V_{ds}$ , and an intrinsic damping constant,  $\gamma_i$ . The overall effective temperature of the resonator is then determined by an average of the temperatures of the two baths at temperatures  $T_i$  and  $T_e$ , with weights that depend on the respective damping constants  $\gamma_i$  and  $\gamma_e$ .<sup>14</sup>

The strength of the interaction between the resonator and the SET is conveniently described by the dimensionless parameter  $\kappa = m\omega_0^2 x_0^2 / (eV_{ds})$  and the frequency by  $\epsilon = \omega_0 \tau_t$ , where  $\tau_t = Re/V_{ds}$  is the electron tunnelling time. In terms of these dimensionless parameters, the intrinsic damping rate of the resonator due to interactions with the electrons is<sup>14</sup>  $\gamma_i = \kappa \epsilon^2 / \tau_t$ . The interaction of the resonator with the electrons also leads to a slight renormalization of resonator frequency,  $\epsilon' = \epsilon(1 - \kappa)^{1/2}$ . Finally, the external temperature is conveniently expressed in terms of the drain-source voltage as the dimensionless parameter,  $\Theta = k_B T_e / eV_{ds}$ .

### III. SET CURRENT NOISE

The noise in the current through a SET is generated by the fluctuations in the time dependent current flowing through the system. Since the SET contains more than one tunnel junction, the time-dependent current which flows is not simply the tunnel current across either one of the junctions.<sup>19,21,22,23</sup> When an electron tunnels through either junction, charge also flows in the external circuit connected to the SET island (so that the charge stored in each capacitor returns to its equilibrium value) and hence also contributes to the current. The current flowing through the SET can be measured in either the left or right-hand lead and the average current flowing through the leads must necessarily be the same.

The time dependent current through the gated SET is, in principle, slightly different in the left and right-hand leads, even for the symmetrical case we consider here where the tunnel-junction capacitances,  $C_j$ , are the same.<sup>21</sup> The time dependent current through the left-hand lead can be written<sup>19,21</sup>

$$I^{(L)}(t) = a^{(L)} \dot{Q}_L(t) + b^{(L)} \dot{Q}_R(t), \quad (3)$$

whilst the time dependent current through the right-hand lead is given by<sup>21</sup>

$$I^{(R)}(t) = a^{(R)} \dot{Q}_L(t) + b^{(R)} \dot{Q}_R(t), \quad (4)$$

where  $\dot{Q}_{L(R)}$  are the tunnel currents through the  $L(R)$  junctions respectively, and<sup>21</sup>

$$a^{(L)} = b^{(R)} = \frac{C_j + C_g(x)}{2C_j + C_g(x)} \quad (5)$$

$$b^{(L)} = a^{(R)} = \frac{C_j}{2C_j + C_g(x)}. \quad (6)$$

Notice, however, that the two coefficients  $a^{(i)}$  and  $b^{(i)}$ ,  $i = L, R$ , add up to unity, whichever lead we consider. Because of the dependence of these coefficients on the gate capacitance,  $C_g(x)$ , there will necessarily be a weak dependence of the coefficients on the position of the resonator. However, even the leading order position dependent term in the coefficients will be smaller by a factor  $C_g/C_j$  than those arising within the expressions for the time dependent currents. Since we are treating the case where  $C_g/C_j \ll 1$ , the corrections generated by the position dependence of  $a^{(i)}$  and  $b^{(i)}$ ,  $i = L, R$ , will be neglected here.<sup>24</sup> In fact, it turns out that the noise spectrum is relatively insensitive to the exact values of the coefficients, and hence which lead the current is measured in. Therefore, for simplicity, we will not distinguish between the two leads in what follows and set  $a^{(L)} = a^{(R)} = a$ , and  $b^{(L)} = b^{(R)} = b$ .

The current fluctuations in the SET are constrained by the conservation of charge. Charge conservation implies that the charge that has tunneled through the left-hand junction in time  $t$ ,  $Q_L(t)$ , and the charge that has tunneled through the right junction in the same period,  $Q_R(t)$  must be connected by the relation

$$Q_L(t) - Q_R(t) = Q_D(t) \quad (7)$$

where  $Q_D(t)$  is the charge dwelling on the island between the two barriers at time  $t$ . Furthermore, since the average tunnel currents through the left- and right-hand junctions are the same, they are both also equal to the average current through the SET,<sup>14</sup>

$$\langle I \rangle = \langle \dot{Q}_L \rangle = \langle \dot{Q}_R \rangle, \quad (8)$$

and hence we also have,  $\langle \dot{Q}_D \rangle = 0$ .

The spectrum of current noise in the SET is given by the Fourier transform of the current-current correlation function,<sup>23</sup>

$$S_{II}(\omega) = 2 \int_{-\infty}^{\infty} d\tau K_{II}(\tau) \cos(\omega\tau), \quad (9)$$

where

$$K_{II}(\tau) = \langle I(t+\tau)I(t) \rangle - \langle I(t) \rangle^2. \quad (10)$$

The current-current correlation function,  $K_{II}(\tau)$ , is taken to be independent of  $t$ .

The noise in the total current is a combination of the noise in the tunnel currents through the left and right-hand junctions,  $S_{I_L I_L}(\omega)$  and  $S_{I_R I_R}(\omega)$  respectively, and the charge noise of the SET island  $S_Q(\omega)$ . Using the expression for the full current in terms of tunnel currents through the two junctions and the charge conservation relation, we can write the current noise spectrum as a sum of the three terms:<sup>25</sup>

$$S_{II}(\omega) = aS_{I_L I_L}(\omega) + bS_{I_R I_R}(\omega) - ab\omega^2 S_Q(\omega), \quad (11)$$

where

$$S_{I_L I_L}(\omega) = 2 \int_{-\infty}^{\infty} d\tau \cos(\omega\tau) \left[ \langle \dot{Q}_L(t+\tau)\dot{Q}_L(t) \rangle - \langle \dot{Q}_L(t) \rangle^2 \right] \quad (12)$$

$$S_{I_R I_R}(\omega) = 2 \int_{-\infty}^{\infty} d\tau \cos(\omega\tau) \left[ \langle \dot{Q}_R(t+\tau)\dot{Q}_R(t) \rangle - \langle \dot{Q}_R(t) \rangle^2 \right] \quad (13)$$

$$\omega^2 S_Q(\omega) = 2 \int_{-\infty}^{\infty} d\tau \cos(\omega\tau) \langle \dot{Q}_D(t+\tau)\dot{Q}_D(t) \rangle. \quad (14)$$

In the last equation, the SET island charge noise,  $S_Q(\omega)$ , is identified with the noise in  $\dot{Q}_D(t)$  (this connection will be derived in Sec. V). Notice that the charge noise acts to reduce the full noise spectrum, compared to the individual tunnel current noise spectra, reflecting the well-known fact that current noise is suppressed in double barrier structures.<sup>19</sup>

The zero-frequency noise of the tunnel currents through the two junctions are equal, because of charge conservation, and hence  $S_{II}(0) = S_{I_L I_L}(0) = S_{I_R I_R}(0)$ . However, in order to obtain the full current noise at finite frequency we must calculate each of its three components. The noise in the tunnel currents  $S_{I_L I_L}(\omega)$  and  $S_{I_R I_R}(\omega)$  are obtained first, using an equation of motion method, then the charge noise,  $S_Q(\omega)$  is calculated using a similar approach. The three elements of the current noise are then combined to obtain the full spectrum.

#### IV. TUNNEL CURRENT NOISE SPECTRA

The noise in the tunnel current across the SET junctions can be calculated using an approach due to MacDonald<sup>26,27</sup> which relies on the fact that the number of charges that have passed across the junction as a function of time can be counted. For the SET-resonator system, the description in terms of a probability distribution is easily extended to record the number of electrons passing across one or other of the tunnel barriers linking the SET island to the leads.

Starting with the left-hand junction, we follow MacDonald<sup>26,27</sup> in introducing the statistically stationary variable,

$$\dot{\tilde{Q}}_L = \dot{Q}_L - \langle \dot{Q}_L \rangle \quad (15)$$

and write,

$$S_{I_L I_L}(\omega) = 2\omega \int_0^\infty \frac{\partial \langle \tilde{Q}_L^2(\tau) \rangle}{\partial \tau} \sin(\omega\tau) d\tau \quad (16)$$

where,

$$\langle \tilde{Q}_L^2(\tau) \rangle = \left\langle \left[ \int_t^{t+\tau} \dot{Q}_L(t') dt' \right]^2 \right\rangle \quad (17)$$

$$= \left\langle \left[ \int_t^{t+\tau} \dot{Q}_L(t') dt' - \langle \dot{Q}_L \rangle \tau \right]^2 \right\rangle \quad (18)$$

$$= e^2 \langle n^2(\tau) \rangle - I_0^2 \tau^2 \quad (19)$$

with  $n(\tau)$  the number of electrons which passed across the left-hand junction in time  $\tau$  and  $I_0 = \langle I \rangle = \langle \dot{Q}_L \rangle$ , the average current. The MacDonald approach has been used to calculate the current-noise in a number of mesoscopic systems<sup>28,29</sup> and the subtleties of the method are described particularly carefully by Ruskov and Korotkov.<sup>28</sup>

The probability distributions for the SET-resonator system are readily generalized to include the number of electrons that have passed through either one of the junctions. In order to calculate the noise in the current through the left-hand junction, we define  $P_{N(N+1)}^n(x, u; t)$  as the probability that, after time  $t$ ,  $n$  electrons have passed across the left-hand junction, there are  $N(N+1)$  electrons on the SET island and the resonator is at position  $x$  with velocity  $u$ . The master equations [Eqs. (1) and (2)] now take the modified form

$$\frac{\partial P_N^n}{\partial t} = \omega_0^2 x \frac{\partial P_N^n}{\partial u} - u \frac{\partial P_N^n}{\partial x} + \frac{\partial}{\partial u} \left( \gamma_e u P_N^n + \frac{G}{2m^2} \frac{\partial P_N^n}{\partial u} \right) + \left( \Gamma_L P_{N+1}^{n-1} - \Gamma_R P_N^n - \frac{m\omega_0^2 x_0}{Re^2} x [P_{N+1}^{n-1} + P_N^n] \right) \quad (20)$$

$$\frac{\partial P_{N+1}^n}{\partial t} = \omega_0^2 (x - x_0) \frac{\partial P_{N+1}^n}{\partial u} - u \frac{\partial P_{N+1}^n}{\partial x} + \frac{\partial}{\partial u} \left( \gamma_e u P_{N+1}^n + \frac{G}{2m^2} \frac{\partial P_{N+1}^n}{\partial u} \right) - \left( \Gamma_L P_{N+1}^n - \Gamma_R P_N^n - \frac{m\omega_0^2 x_0}{Re^2} x P_{N+1}^n \right) \quad (21)$$

where  $P^n(x, u; t) = P_N^n(x, u; t) + P_{N+1}^n(x, u; t)$ . Notice that only the terms which describe the transition from charge state  $N+1$  to  $N$  with an electron tunnelling out through the left junction couple to a change in  $n$ .

The rate of change of the average of the squared number of charges passing through the left-hand junction in time  $\tau$  is given by<sup>28</sup>

$$\frac{d \langle n^2(\tau) \rangle}{d\tau} = \sum_n n^2 \int dx \int du \left[ \dot{P}_{N+1}^n(x, u; \tau) + \dot{P}_N^n(x, u; \tau) \right] \quad (22)$$

$$= 2 \left( \Gamma_L \langle n \rangle_{N+1} - \frac{m\omega_0^2 x_0}{Re^2} \langle xn \rangle_{N+1} \right) + \frac{I_0}{e}, \quad (23)$$

where we have re-ordered the sum over  $n$  in the first term, and substituted from Eqs. (20) and (21). The averages  $\langle \dots \rangle_{N+1}$ , are with respect to the sub-ensemble of systems with  $N+1$  charges on the SET island, i.e.

$$\langle \dots \rangle_{N+1} = \sum_n \int dx \int du (\dots) P_{N+1}^n(x, u; \tau).$$

The initial conditions for the distributions,  $P_{N(N+1)}^n(x, u; \tau = 0)$ , are given by the corresponding steady-state distributions for the SET-resonator system,<sup>14</sup>  $P_{N(N+1)}^{(s)}(x, u)$ ,

$$P_{N(N+1)}^n(x, u; \tau = 0) = \delta_{n,0} P_{N(N+1)}^{(s)}(x, u),$$

and hence we have

$$\sum_n P_{N(N+1)}^n(x, u; \tau) = P_{N(N+1)}^{(s)}(x, u),$$

for all  $\tau$ .

The overall expression for the noise in the current through the left-hand junction is given by

$$S_{I_L I_L}(\omega) = 2\omega \int_0^\infty \left\{ 2 \left[ e^2 \left( \Gamma_L \langle n \rangle_{N+1} - \frac{\kappa \langle xn \rangle_{N+1}}{\tau_t x_0} \right) - I_0^2 \tau \right] + e I_0 \right\} \sin(\omega\tau) d\tau. \quad (24)$$

The quantities  $\langle n(\tau) \rangle_{N+1}$  and  $\langle xn(\tau) \rangle_{N+1}$  can be obtained by deriving their equations of motion and those of the other average quantities they couple to. The equations of motion for moments of the form  $\langle x^p u^q n \rangle$  and  $\langle x^p u^q n \rangle_{N+1}$  are given by

$$\frac{d}{d\tau} \langle x^p u^q n \rangle = \sum_n \int dx \int du x^p u^q n \left[ \dot{P}_{N+1}^n(x, u; \tau) + \dot{P}_N^n(x, u; \tau) \right], \quad (25)$$

$$\frac{d}{d\tau} \langle x^p u^q n \rangle_{N+1} = \sum_n \int dx \int du x^p u^q n \dot{P}_{N+1}^n(x, u; \tau) \quad (26)$$

respectively. Substituting for  $\dot{P}_{N+1(N)}^n(x, u; \tau)$  from the appropriate master equation [Eqns. (20) and (21)], we can derive the closed set of equations,

$$\frac{d}{d\tau} \langle n \rangle_{N+1} = \frac{I_0}{e} \Gamma_R \tau - (\Gamma_L + \Gamma_R) \langle n \rangle_{N+1} + \frac{m\omega_0^2 x_0}{Re^2} \langle xn \rangle \quad (27)$$

$$\frac{d}{d\tau} \langle xn \rangle = \langle un \rangle + \Gamma_L \langle x \rangle_{N+1} - \frac{m\omega_0^2 x_0}{Re^2} \langle x^2 \rangle_{N+1} \quad (28)$$

$$\frac{d}{d\tau} \langle un \rangle = -\omega_0^2 [\langle xn \rangle - x_0 \langle n \rangle_{N+1}] - \frac{m\omega_0^2 x_0}{Re^2} \langle ux \rangle_{N+1} + \Gamma_L \langle u \rangle_{N+1} - \gamma_e \langle un \rangle \quad (29)$$

$$\frac{d}{d\tau} \langle xn \rangle_{N+1} = \langle un \rangle_{N+1} + \Gamma_R \langle xn \rangle - (\Gamma_L + \Gamma_R) \langle xn \rangle_{N+1} + \frac{m\omega_0^2 x_0}{Re^2} \langle x^2 n \rangle \quad (30)$$

$$\frac{d}{d\tau} \langle un \rangle_{N+1} = -\omega_0^2 [\langle xn \rangle_{N+1} - x_0 \langle n \rangle_{N+1}] + \Gamma_R \langle un \rangle + \frac{m\omega_0^2 x_0}{Re^2} \langle xun \rangle - (\Gamma_L + \Gamma_R) \langle un \rangle_{N+1} - \gamma_e \langle un \rangle_{N+1} \quad (31)$$

$$\frac{d}{d\tau} \langle x^2 n \rangle = 2 \langle xun \rangle + \Gamma_L \langle x^2 \rangle_{N+1} - \frac{m\omega_0^2 x_0}{Re^2} \langle x^3 \rangle_{N+1} \quad (32)$$

$$\frac{d}{d\tau} \langle u^2 n \rangle = -2\omega_0^2 [\langle xun \rangle - x_0 \langle un \rangle_{N+1}] + \Gamma_L \langle u^2 \rangle_{N+1} - \frac{m\omega_0^2 x_0}{Re^2} \langle u^2 x \rangle_{N+1} - 2\gamma_e \langle u^2 n \rangle + \frac{I_0 G}{em^2} \tau \quad (33)$$

$$\frac{d}{d\tau} \langle xun \rangle = -\omega_0^2 [\langle x^2 n \rangle - x_0 \langle nx \rangle_{N+1}] + \langle u^2 n \rangle + \Gamma_L \langle xu \rangle_{N+1} - \frac{m\omega_0^2 x_0}{Re^2} \langle x^2 u \rangle_{N+1} - \gamma_e \langle xun \rangle. \quad (34)$$

The averages which do not involve  $n$  are constants (i.e. independent of  $\tau$ ) and are evaluated for the steady-state distributions,  $P_{N(N+1)}^{(s)}(x, u)$ .<sup>28</sup> The details of the evaluation of these averages are given in Appendix A.

The set of coupled differential equations [Eqns. (27-34)] is readily integrated numerically to give  $\langle n \rangle_{N+1}$  and  $\langle xn \rangle_{N+1}$ , from which the left-hand junction current noise spectrum can be obtained. Since we are interested in the number of electrons passing through the left-hand junction in a time  $\tau$ , all quantities involving  $n$  will clearly be set to zero at  $\tau = 0$ .<sup>28</sup>

Integrating the equations of motion for  $\langle n \rangle_{N+1}$  and  $\langle xn \rangle_{N+1}$  and performing the Fourier integral numerically<sup>30</sup> (incorporating an appropriate long-time cut-off), we can obtain the current-noise spectrum,  $S_{I_L I_L}(\omega)$  for various choices of the system parameters. The current noise with the coupling to the resonator set to zero,  $S_{I_L I_L}^0(\omega)$ , can also be calculated analytically for comparison,<sup>23</sup>

$$S_{I_L I_L}^0(\omega) = 2\omega I_0 \int_0^\infty d\tau \sin(\omega\tau) \left[ e + \frac{2I_0}{\Gamma_L + \Gamma_R} \left( e^{-(\Gamma_L + \Gamma_R)\tau} - 1 \right) \right] \quad (35)$$

$$= 2eI_0 - \frac{4I_0^2(\Gamma_L + \Gamma_R)}{(\Gamma_L + \Gamma_R)^2 + \omega^2}. \quad (36)$$

Initially, we consider the simplest case, where there is no external damping and the resonator substrate is at zero temperature (i.e.  $\gamma_e \tau_t = 0$  and  $\Theta = 0$ ), and examine the dependence of the tunnel current noise spectrum on the resonator frequency and the strength of the coupling to the SET. Figure 2 shows  $S_{I_L I_L}(\omega)$  for several choices of the dimensionless coupling and frequency parameters,  $\kappa$  and  $\epsilon$ .<sup>31</sup> For ease of comparison, the frequency axis is scaled by the renormalized resonator frequency,  $\Omega = \omega \tau_t / \epsilon'$ . The spectra are dominated by sharp, asymmetric, peaks arising at  $\Omega = 0$ , the renormalized resonator frequency  $\Omega = 1$  and at twice that frequency,  $\Omega = 2$ . None of these three features appear in the current noise spectrum for a SET without a resonator. At high frequencies, beyond the range shown in Fig. 2, all of the spectra reduce to the usual single-junction value  $2eI_0$ .

The effect of the resonator on the noise spectrum depends on both the strength of the coupling between the resonator position and the SET junction tunnel rates, measured by  $\kappa$ , as well as the underlying dynamics of the resonator, which in the absence of extrinsic temperature or damping, is conveniently parameterized by  $\gamma_i \tau_t = \kappa \epsilon^2$ .

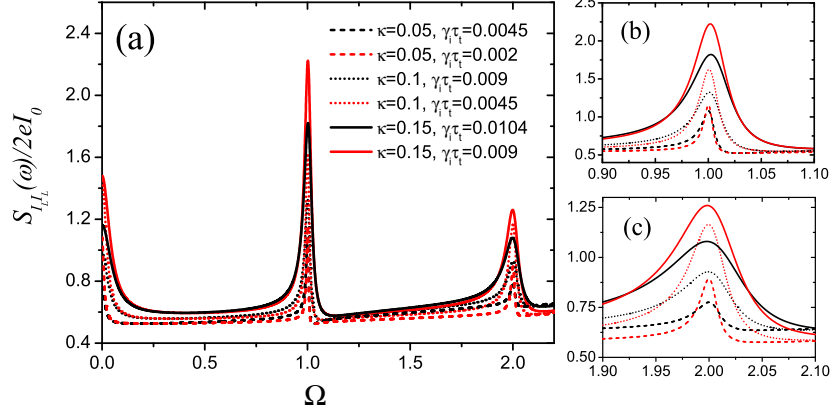


FIG. 2: Current noise spectrum of the left-hand junction,  $S_{I_L I_L}(\omega)$ , for a range of resonator parameters as a function of the scaled frequency  $\Omega = \omega\tau_t/\epsilon'$ . The full spectrum is shown in (a) while the insets (b) and (c) show the details of the peaks at  $\Omega = 1$  and  $2$ , respectively. All calculations are performed for  $\gamma_e\tau_t = \Theta = 0$  and  $\Gamma_L = \Gamma_R$ .

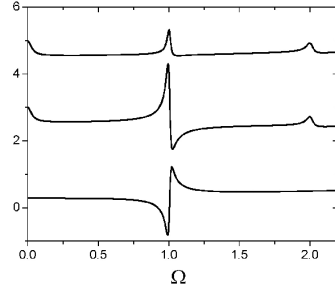


FIG. 3: Comparison of the contributions to the left-hand junction current noise due to the  $\langle xn \rangle_{N+1}$  and  $\langle n \rangle_{N+1}$  terms in Eq. (23), given by  $F(\omega)$  and  $G(\omega)$  respectively. The curves have been displaced vertically for clarity. From top to bottom, the curves are:  $S_{I_L I_L}(\omega)/(2eI_0)$ ,  $F(\omega)$  and  $G(\omega)$ . In each case  $\kappa = 0.1$ ,  $\epsilon = 0.3$ ,  $\gamma_e\tau_t = \Theta = 0$  and  $\Gamma_L = \Gamma_R$ .

The coupling strength,  $\kappa$ , plays a dual role as it controls both the amount by which the resonator motion alters the electron tunnel rates, and the resonator dynamics through the intrinsic damping  $\gamma_i$ . Fig. 2 shows that the heights of the peaks depend sensitively on both  $\kappa$  and  $\gamma_i$ . The peak heights increase with an increase in  $\kappa$ , at fixed  $\gamma_i$ , whilst an increase in  $\gamma_i$  at fixed  $\kappa$  (i.e. an increase in  $\epsilon$ ) reduces the heights of the peaks. Notice, however, that the peaks at  $\Omega = 0$  and  $2$  reduce more strongly as  $\gamma_i$  increases than the one at  $\Omega = 1$ .

We can understand the origin of the features in the current noise spectrum by splitting it into its two constituent parts: that arising from  $\langle n \rangle_{N+1}$  and that from  $\langle xn \rangle_{N+1}$ . Figure 3 shows a noise spectrum for a particular choice of parameters ( $\kappa = 0.1$ ,  $\epsilon = 0.3$ ), and the two functions  $F(\omega)$  and  $G(\omega)$ , which add to give the noise spectrum

$$\frac{S_{I_L I_L}(\omega)}{2eI_0} = F(\omega) + G(\omega). \quad (37)$$

The functions  $F(\omega)$  and  $G(\omega)$  are essentially the Fourier integrals of  $\langle xn \rangle_{N+1}$  and  $\langle n \rangle_{N+1}$ , respectively, with the appropriate linear and constant terms subtracted off in each case. Written out explicitly, they have the form

$$F(\omega) = \frac{2\omega}{I_0} \int_0^\infty d\tau \left[ \frac{\kappa}{2} I_0 - \frac{\kappa}{\tau_t} \left( e \frac{\langle xn \rangle_{N+1}}{x_0} - \alpha\tau \right) \right] \sin(\omega\tau) \quad (38)$$

$$G(\omega) = \frac{2\omega}{I_0} \int_0^\infty d\tau \left[ \frac{(1-\kappa)}{2} I_0 + \Gamma_L (e \langle n \rangle_{N+1} - \alpha\tau) \right] \sin(\omega\tau), \quad (39)$$

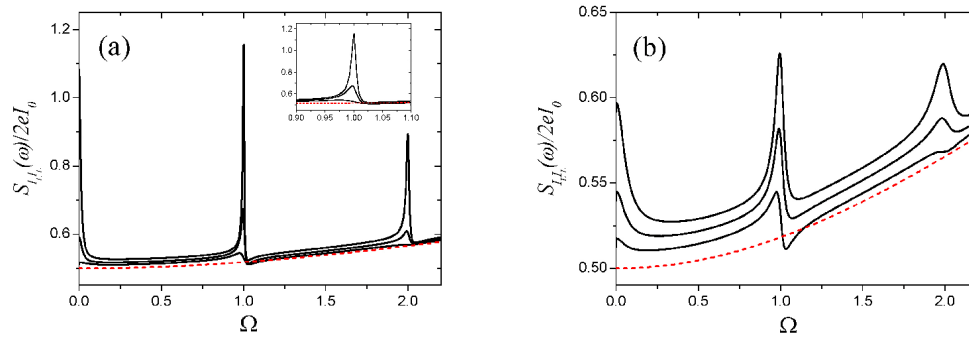


FIG. 4: Effects of finite extrinsic damping and temperature on the current noise through the left-hand junction,  $S_{I_L I_L}(\omega)$ , for the coupled system with  $\kappa = 0.05$ ,  $\epsilon = 0.2$ . Panel (a) shows the noise spectra for  $\gamma_e = 0$  (upper curve),  $\gamma_e = \gamma_i$  (middle curve) and  $\gamma_e = 5\gamma_i$  (lower curve), with  $\Theta = 0$  in each case. Panel (b) shows the noise spectra for  $\Theta = 0.2$  (upper curve),  $\Theta = 0.1$  (middle curve) and  $\Theta = 0$  (lower curve) with  $\gamma_e = 5\gamma_i$  in each case. In both plots the corresponding noise spectrum for the uncoupled system is shown as a dashed curve. All calculations are performed for  $\Gamma_L = \Gamma_R$ .

with

$$\alpha = \frac{I_0^2}{e(\Gamma_L - \kappa/\tau_t)}. \quad (40)$$

The function  $G(\omega)$ , which contains the  $\langle n \rangle_{N+1}$  term, has a single feature, at the renormalized resonator frequency. In contrast, the function  $F(\omega)$ , which contains the  $\langle xn \rangle_{N+1}$  term, has three features: one at  $\Omega = 0$ , one at the renormalized frequency,  $\Omega = 1$ , and one at  $\Omega = 2$ . We can understand these features in terms of non-trivial correlations between the variables  $x$  and  $n$ . From the spectrum  $G(\omega)$ , we see that the  $n$  term has a component oscillating at frequency  $\epsilon'$  and since  $x$  will also oscillate at the same frequency, it is not surprising that the combination of the two dynamical variables in the term  $\langle xn \rangle_{N+1}$  gives rise to a component oscillating at  $2\epsilon'$  as well as at  $\epsilon'$ . The explicit dependence on  $x$  in  $\langle xn \rangle_{N+1}$  also makes the features in  $F(\omega)$  more sensitive to the magnitude of  $\gamma_i$  than those in  $G(\omega)$ . Hence in the full spectrum the peaks that are due to  $\langle xn \rangle_{N+1}$  alone (at  $\Omega = 0, 2$ ) reduce more rapidly with increasing  $\gamma_i$  than the one with contributions from  $\langle xn \rangle_{N+1}$  and  $\langle n \rangle_{N+1}$  (at  $\Omega = 1$ ).

The enhancement of the low frequency noise is to be expected because of the effective correlations between successive electrons induced by the interactions with the resonator. It is known from other contexts<sup>32</sup> that zero-frequency noise can be increased when an electron tunnelling event is able to change the internal state of a mesoscopic system (such as a quantum dot). In this case, an electron passing through the SET alters the state of the resonator, which in turn alters the tunnelling rates for subsequent electrons. However, any excitation of the resonator is damped out over time and hence the zero-frequency peak in the spectrum follows a very similar pattern to the other peaks: it increases with the coupling strength,  $\kappa$ , but reduces with increasing damping,  $\gamma_i$ .

It is the approximation of the gate capacitance by the linear form,  $C_g(x) \simeq C_g(1 - x/d)$ , which means that there are no further peaks in the current noise beyond that at  $\Omega = 2$ . If higher order terms had been included in the expression for the gate capacitance then they would have led to higher order terms in the position dependence of the tunnel rates, which we would expect to generate peaks at higher multiples of the resonator frequency. However, within the regime we consider here, where  $x/d \ll 1$ , the additional peaks at higher frequency would be much smaller than those at  $\Omega = 1$  and 2.

The effects of extrinsic damping and finite background temperature on the tunnel current noise spectrum are illustrated in Fig. 4, with the appropriate noise spectrum for the uncoupled system shown for comparison. It is clear that a non-zero value of  $\gamma_e$  rounds down each of the peaks at  $\Omega = 0, 1$  and 2. Furthermore, the peaks at  $\Omega = 1$  and 2 are also shifted to slightly lower frequencies, reflecting the fact that the extrinsic damping causes an extra reduction in the resonator frequency (beyond that due to the interaction with the electrons). The influence of extrinsic damping gradually fades at higher frequencies where the spectrum is hardly affected by the resonator anyway. A non-zero background temperature counteracts the damping, increasing the height and broadening the peaks.

The comparison with the uncoupled case in Fig. 4, also reveals a small suppression of the noise just after the peak at  $\Omega = 1$ , and a similar feature after the peak at  $\Omega = 2$ . We can understand the presence of this suppression in a loose way by considering the actual motion of the resonator as a competition between two components. Firstly, we can consider a resonator coupled to a thermal bath, in this case the mechanical motion would fluctuate strongly leading to an enhancement of the noise at the mechanical frequency.<sup>18</sup> Of course these thermal-like fluctuations arise already



from the interaction between the resonator and the electrons,<sup>14</sup> and are increased by the presence of an extrinsic bath. However, it seems likely that the interaction between the electrons and the resonator must also induce some coordination between the electronic and mechanical motion which would tend to make the current flow more regular and hence suppress the noise, at least at the resonator frequency. As we would expect from this simple picture, Fig. 4b shows that increasing the background temperature rapidly washes out the regions of noise suppression.

The noise in the current through the right-hand junction can be obtained in exactly the same manner as that through the left-hand junction. Using MacDonald's formula, we have

$$S_{I_R I_R}(\omega) = 2\omega \int_0^\infty \left\{ 2 \left[ e^2 \left( \Gamma_R \langle n \rangle_N + \frac{\kappa}{\tau_t} \frac{\langle xn \rangle_N}{x_0} \right) - I_0^2 \tau \right] + eI_0 \right\} \sin(\omega\tau) d\tau, \quad (41)$$

where in this case  $n(\tau)$  is the number of electrons to pass through the *right-hand* junction in time  $\tau$ .

The master equations [Eqs. (1) and (2)] are also readily modified to include the number of electrons tunnelling (from right to left) across the right-hand junction. A closed set of equations of motion that allow  $\langle n \rangle_N$  and  $\langle xn \rangle_N$  to be determined by numerical integration are obtained following the same procedure as that used for the left-hand junction.

Carrying out the numerical integration and then the Fourier integral, as before, we can compare the resulting noise spectrum through the right-hand junction with that through the left-hand junction. As would be expected for the very symmetrical SET layout we consider here, the current noise spectra of the two junctions are very similar, but away from  $\Omega = 0$  they are not identical. In fact, the magnitudes of the peaks in the left and right-hand tunnel noise spectra at  $\Omega = 1, 2$  differ by up to a few percent for the parameters used here. The differences in the two spectra arise because the resonator breaks the overall symmetry of the circuit.

## V. CHARGE NOISE ON THE SET ISLAND

Apart from the contributions due to the tunnel currents across the two SET junctions, the full current-noise spectrum also contains a contribution arising from fluctuations in the charge stored on the SET island,

$$\omega^2 S_Q(\omega) = 2 \int_{-\infty}^\infty d\tau \cos(\omega\tau) \langle \dot{Q}_D(t+\tau) \dot{Q}_D(t) \rangle. \quad (42)$$

The average charge on the SET island is a constant (i.e.  $\langle \dot{Q}_D \rangle = 0$ ), thus we can use MacDonald's formula to show explicitly that this term is indeed the charge noise spectrum,

$$S_Q(\omega) = 2\omega^{-1} \int_0^\infty \frac{\partial \langle Q_D(\tau)^2 \rangle}{\partial \tau} \sin(\omega\tau) d\tau \quad (43)$$

$$= 4 \int_0^\infty d\tau \cos(\omega\tau) [\langle Q_D(t+\tau) Q_D(t) \rangle - \langle Q_D^2 \rangle], \quad (44)$$

where an integration by parts has been performed.

Within our model of the SET, the excess charge can only be either zero or one electron, hence  $\langle Q_D^2 \rangle = -e \langle Q_D \rangle$ . Since  $\langle Q_D(t) \rangle$  is simply the average occupancy of the SET island multiplied by the electronic charge,  $-e$ , we can use the master equations to write down a closed set of coupled equations that link the average excess charge, position,  $\langle x \rangle$ , and velocity,  $\langle u \rangle$ , of the resonator,

$$\frac{d}{dt} \langle Q_D(t) \rangle = -e\Gamma_R - \frac{V_{ds}}{eR} \langle Q_D(t) \rangle - \frac{m\omega_0^2 x_0}{eR} \langle x(t) \rangle \quad (45)$$

$$\frac{d}{dt} \langle x(t) \rangle = \langle u(t) \rangle \quad (46)$$

$$\frac{d}{dt} \langle u(t) \rangle = -\omega_0^2 \langle x(t) \rangle - \frac{\omega_0^2 x_0}{e} \langle Q_D(t) \rangle - \gamma_e \langle u(t) \rangle. \quad (47)$$

Note that these equations are equivalent to the mean-coordinate equations derived in Ref. 14.

Since the equations of motion for the probability distribution are Markovian, the equations of motion for two-time correlation functions of the charge can be obtained from the equations for the average quantities [Eqs. (45-47)] using the regression theorem.<sup>33</sup> Thus we obtain,

$$\frac{d}{dt} \langle Q_D(t+\tau) Q_D(t) \rangle = -e\Gamma_R \langle Q_D(t) \rangle - \frac{V_{ds}}{eR} \langle Q_D(t+\tau) Q_D(t) \rangle - \frac{m\omega_0^2 x_0}{eR} \langle x(t+\tau) Q_D(t) \rangle \quad (48)$$

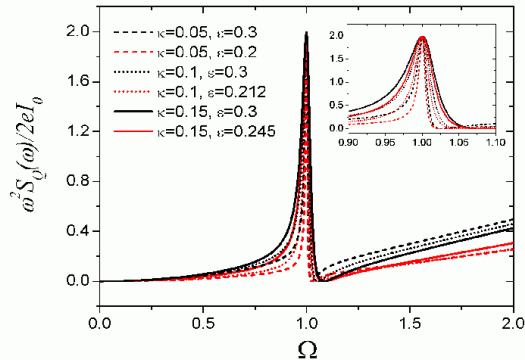


FIG. 5: Frequency scaled charge noise spectrum,  $\omega^2 S_Q(\omega)$ , for a range of resonator parameters, with  $\gamma_e \tau_t = \Theta = 0$  and  $\Gamma_L = \Gamma_R$ .

$$\frac{d}{d\tau} \langle x(t+\tau) Q_D(t) \rangle = \langle u(t+\tau) Q_D(t) \rangle \quad (49)$$

$$\frac{d}{d\tau} \langle u(t+\tau) Q_D(t) \rangle = -\omega_0^2 \langle x(t+\tau) Q_D(t) \rangle - \frac{\omega_0^2 x_0}{e} \langle Q_D(t+\tau) Q_D(t) \rangle - \gamma_e \langle u(t+\tau) Q_D(t) \rangle. \quad (50)$$

The initial conditions (at  $\tau = 0$ ) are given by the steady state properties of the system. The charge noise spectrum is then obtained by integrating the coupled equations to obtain  $\langle Q_D(t+\tau) Q_D(t) \rangle$ , and then performing the necessary Fourier integral.

The frequency scaled spectrum,  $\omega^2 S_Q(\omega)$ , is shown in Fig. 5 for a range of resonator couplings and frequencies. The charge noise spectrum of the SET island, like the function  $G(\omega)$  considered earlier, contains only a single peak, at the renormalized resonator frequency. This is not surprising as the equations of motion from which  $S_Q(\omega)$  is obtained [Eqs. (48-50)] have a structure which is very similar to those which determine  $G(\omega)$  [Eqs. (27-29)]. Figure 5 shows that the height of the  $\Omega = 1$  peak in  $\omega^2 S_Q(\omega)$  is almost independent of  $\kappa$  and  $\epsilon$  (provided  $\kappa$  and  $\epsilon$  are much less than unity, and also non-zero), this is because the peak height in the charge noise itself is approximately determined by the ratio of the coupling to the intrinsic damping  $\kappa/(\gamma_i \tau_t) = 1/\epsilon^2$ .<sup>34</sup>

## VI. FULL CURRENT NOISE SPECTRUM

Once the noise spectra of the tunnel currents and the charge on the island have been calculated, the full current-noise spectrum is readily obtained by combining its components in the appropriate way [as given by Eq. (11)]. Figure 6 shows the full current-noise spectrum for the particular choice of the parameters  $a = b$ . The overall spectrum is dominated by peaks at  $\Omega = 0, 1$  and  $2$ , and largely flat elsewhere. The peak in the charge noise spectrum suppresses the peak in the tunnel noise spectra at  $\Omega = 1$ , so that the peak at  $\Omega = 2$  can become larger in the overall spectrum. For a combination of sufficiently strong coupling and weak damping, the zero-frequency noise exceeds the Poissonian value  $2eI_0$ .

In the limit where  $\kappa$  goes to zero, the full current noise spectrum is readily obtained analytically. In this limit the left and right-hand junction current noise spectra are the same, and the full current noise (spectrum assuming  $a = b$ ) is

$$S_{II}^0(\omega) = eI_0 \left[ 1 + \left( 1 - \frac{4\Gamma_L \Gamma_R}{\Gamma^2} \right) \frac{\Gamma^2}{\Gamma^2 + \omega^2} \right], \quad (51)$$

where  $\Gamma = \Gamma_L + \Gamma_R$ . This is of course the usual result for sequential tunnelling through a symmetric double-barrier structure.<sup>22,23</sup> Thus in strong contrast to the coupled system, the current noise of the uncoupled, symmetric ( $\Gamma_R = \Gamma_L$ ), SET would be flat:  $S_{II}^0(\omega)/(2eI_0) = 0.5$ .

Figure 6 shows in detail the dependence of the spectrum on the resonator coupling,  $\kappa$  and intrinsic damping  $\gamma_i \tau_t = \kappa \epsilon^2$ . Once the frequency of the spectra is scaled by the renormalized frequency, a relatively simple behavior emerges. Increasing the coupling strength increases the height and widths of the peaks, whilst increasing  $\gamma_i$  (for fixed coupling) simply rounds the peaks down without affecting their widths. Although the heights of the peaks at  $\Omega = 1$  and  $2$  scale with coupling in a very similar way in the individual tunnel current spectra (see Fig. 2), the relative

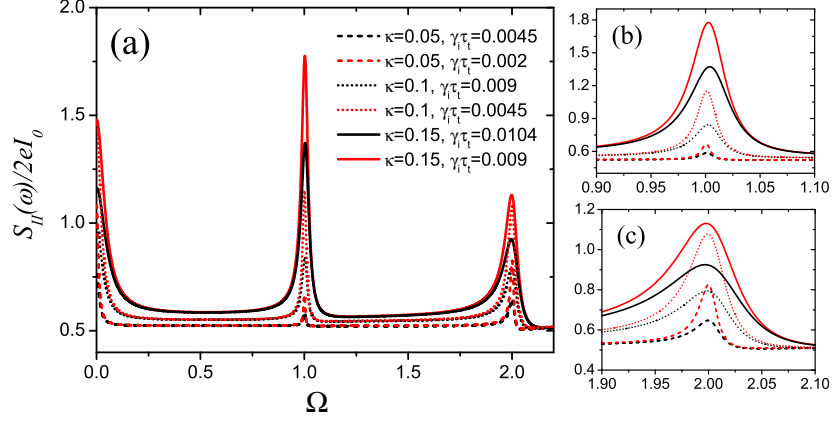


FIG. 6: Full current noise spectrum,  $S_{II}(\omega)$ , for a range of resonator parameters, assuming  $a = b$  with  $\Theta = 0$ ,  $\gamma_e \tau_t = 0$ . The full spectrum is shown in (a) while the insets (b) and (c) show the details of the peaks at  $\Omega = 1$  and  $2$ , respectively. All calculations are performed for  $\Gamma_L = \Gamma_R$ .

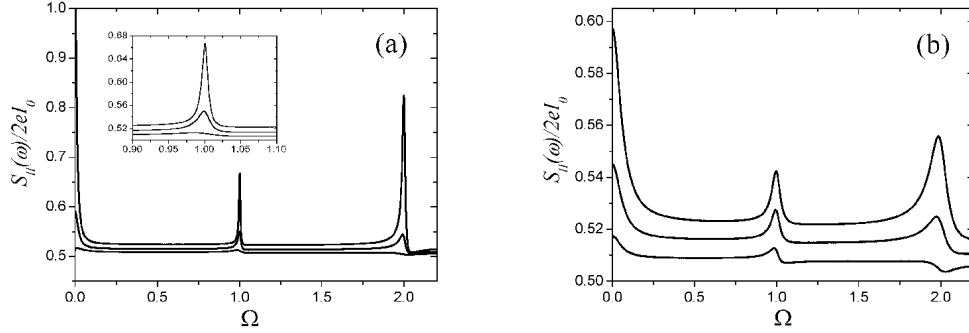


FIG. 7: Full current noise spectrum including extrinsic effects. The influence of extrinsic damping at  $\Theta = 0$  are shown in (a) where the curves (from top to bottom) are for  $\gamma_e = 0$ ,  $\gamma_i$  and  $5\gamma_i$ . The effect of a finite background temperature is shown in (b) where the curves (from top to bottom) are for  $\Theta = 0.2, 0.1$  and  $0$ , and  $\gamma_e = 5\gamma_i$  in each case. The calculations are performed for  $\kappa = 0.05$ ,  $\epsilon = 0.2$ ,  $a = b$  and  $\Gamma_L = \Gamma_R$ .

magnitudes of the peaks at  $\Omega = 1$  and  $\Omega = 2$  in the full spectrum are very sensitive to the magnitude of  $\kappa$ . This is because the peak in the frequency-scaled charge noise  $\omega^2 S_Q(\omega)$  is almost completely insensitive to changes in  $\kappa$  and hence gives rise to a proportionately stronger suppression of the  $\Omega = 1$  peak for smaller  $\kappa$  values.

For the relatively low frequencies shown in Fig. 6, the noise is higher than the uncoupled value, even away from the immediate vicinity of the peaks. This increase in the background noise level depends on  $\kappa$ , but not  $\epsilon$ , and occurs because the resonator breaks the symmetry of the tunnel rates through the two junctions. Only for the uncoupled system do the physical tunnel rates correspond to the parameters  $\Gamma_L$  and  $\Gamma_R$ . When the coupling to the resonator is switched on, the tunnel rates for both junctions depend linearly on the position of the resonator, but with opposite sign, and the strength of this coupling is given by  $\kappa$ . The coupling to the resonator can thus be thought of as giving rise to an effective renormalization of the tunnel rates and since the noise is a minimum for the symmetric tunnel rates of the uncoupled system,  $\Gamma_L = \Gamma_R$  (which we choose here), the coupling always gives rise to an increased background noise level. Although it is not shown in the figures, the current noise reduces to the uncoupled value at large frequencies,  $\Omega \gg 1$ , since any asymmetry in the junction tunnel rates becomes unimportant at large frequencies.

The influence of extrinsic effects on the current noise spectrum are illustrated in Fig. 7. As with the tunnel current spectra, extrinsic damping reduces the peak heights and the background noise level, whilst increasing the background temperature has the opposite effect. Furthermore, it is interesting to note that extrinsic effects can alter the relative heights of the peaks at  $\Omega = 1$  and  $2$ .

The full noise spectrum could equally well be calculated for a variety of cases where  $a \neq b$ , reflecting the balance of

capacitances in the system more accurately, as discussed in Sec. II. However, now that we have obtained the individual spectra of the noise in the tunnel currents and the charge noise, it is clear that for small changes of the coefficients about the values  $a = b = 1/2$ , there would be no qualitative change in the overall current spectrum and so we have not investigated such cases explicitly.

## VII. CONCLUSIONS

The presence of a voltage-gate consisting of a nanomechanical resonator has a dramatic effect on the current-noise spectrum of the SET. The low frequency noise of the SET can be substantially enhanced and two additional peaks appear in the noise spectrum: at the frequency of the resonator (renormalized by the interaction with the SET) and at twice that frequency. Without extrinsic damping and with the background temperature set to zero, the peaks in the current noise are sharp, with heights controlled by the strength of the resonator-SET coupling and the magnitude of the intrinsic damping constant.

The features in the current-noise spectrum reflect the fact that the coupled dynamics of the SET and the resonator lead to important correlations between charges flowing through the SET and the position of the resonator. In particular, the interaction between the resonator and the electrons on the SET island provide a mechanism by which the passage of one electron through the system can affect the motion of subsequent electrons. Hence it is not surprising that the noise in the measured current does not conform to any simple picture based on a combination of the usual noise spectrum of the SET and the mechanical noise spectrum of a damped harmonic oscillator.

The calculation presented here is for the particular case of a classical resonator coupled to a SET as a voltage gate. Very recently a number of other authors have considered aspects of the current noise in a similar nanoelectromechanical system known as the electron shuttle,<sup>1</sup> in both the classical<sup>35,36</sup> and quantum regimes.<sup>37</sup> In particular, the current noise spectrum of a classical shuttle system obtained by Isacsson and Nord<sup>36</sup> shows peaks at the frequency of the mechanical system and its first harmonic in close correspondence with the spectrum of the SET-resonator system described here.

### Acknowledgements

It is a pleasure to thank M.P. Blencowe, A.M. Martin and D.A. Rodrigues for a series of very useful discussions. This work was supported by the EPSRC under grant GR/S42415/01.

## APPENDIX A: CALCULATION OF STEADY-STATE PROPERTIES

The moments of the steady-state distribution which appear in the set of equations of motion describing the motion of charges through the SET [Eqs. (27-34)] can be obtained analytically from the master equations [Eqs. (1) and (2)]. Adding Eqs. (1) and (2) leads to an equation of motion for  $P(x, u; t)$  which in turn can be used to obtain an equation of motion for the moment  $\langle x^n u^k \rangle$ . A similar equation of motion for the moment  $\langle x^n u^k \rangle_{N+1}$  can be obtained directly from Eq. (2).

Assuming a steady state, the equations of motion for  $\langle x^n u^k \rangle$  and  $\langle x^n u^k \rangle_{N+1}$  lead to the following linear equations,

$$k^2 \omega_0^2 [\langle x^{n+1} u^{k-1} \rangle - x_0 \langle x^n u^{k-1} \rangle_{N+1}] = n \langle u^{k+1} x^{n-1} \rangle - k \gamma_e \langle u^k x^n \rangle + k(k-1) \frac{G}{2m^2} \langle u^{k-2} x^n \rangle \quad (\text{A1})$$

$$k^2 \omega_0^2 [\langle x^{n+1} u^{k-1} \rangle_{N+1} - x_0 \langle x^n u^{k-1} \rangle_{N+1}] = n \langle u^{k+1} x^{n-1} \rangle_{N+1} - (k \gamma_e + \Gamma_L + \Gamma_R) \langle u^k x^n \rangle_{N+1} \\ + k(k-1) \frac{G}{2m^2} \langle u^{k-2} x^n \rangle_{N+1} + \Gamma_R \langle u^k x^n \rangle + \frac{m \omega_0^2 x_0}{Re^2} \langle x^{n+1} u^k \rangle, \quad (\text{A2})$$

respectively. By considering these equations for appropriate values of  $k$  and  $n$ , a set of linear equations is generated which can be solved to obtain the necessary steady-state moments, assuming only that the steady-state probability distribution is an even function of the velocity,  $u$ .

---

<sup>1</sup> L.Y. Gorelik, A. Isacsson, M.V. Voinova, B. Kasemo, R.I. Shekhter, and M. Jonson, Phys. Rev. Lett. **80**, 4526. (1998); R.I. Shekhter, Yu. Galperin, L.Y. Gorelik, A. Isacsson, and M. Jonson, J. Phys. Cond. Matt. **15**, R441 (2003).

- <sup>2</sup> A.D. Armour and A. MacKinnon, Phys. Rev. B **66**, 035333 (2002); T. Novotný, A. Donarini and A.-P. Jauho, Phys. Rev. Lett. **90**, 256801 (2003).
- <sup>3</sup> E.M. Weig, R.H. Blick, T. Brandes, J. Kirschbaum, W. Wegscheider, M. Bichler and J.P. Kotthaus, Phys. Rev. Lett. **92**, 046804 (2004).
- <sup>4</sup> N. Nishiguchi, Phys. Rev. B, **68**, R121305 (2003).
- <sup>5</sup> A.N. Cleland and M.L. Roukes, Nature (London) **392**, 160 (1998).
- <sup>6</sup> R.S. Knobel and A.N. Cleland, Nature (London) **424**, 291 (2003).
- <sup>7</sup> M.D. LaHaye, O. Buu, B. Camarota and K.C. Schwab, Science **304**, 74 (2004).
- <sup>8</sup> J. D. White, Jap. J. Appl. Phys. Part 2 **32**, L1571 (1993).
- <sup>9</sup> M.P. Blencowe and M.N. Wybourne, App. Phys. Lett. **77**, 3845 (2000).
- <sup>10</sup> Y. Zhang and M.P. Blencowe, J. Appl. Phys. **91**, 4249 (2002).
- <sup>11</sup> M.F. Bocko and R. Onofrio, Rev. Mod. Phys. **68**, 755 (1996).
- <sup>12</sup> A.D. Armour, M.P. Blencowe and K.C. Schwab, Phys. Rev. Lett. **88**, 148301 (2002).
- <sup>13</sup> M.P. Blencowe, Phys. Rep. **395**, 159 (2004).
- <sup>14</sup> A.D. Armour, M.P. Blencowe and Y. Zhang, Phys. Rev. B **69**, 125313 (2004).
- <sup>15</sup> D. Mozyrsky and I. Martin, Phys. Rev. Lett. **89**, 018301 (2002).
- <sup>16</sup> A. Yu. Smirnov, L.G. Mourkh, and N.J.M. Horing, Phys. Rev. B **67**, 115312 (2003).
- <sup>17</sup> D. Mozyrsky, I. Martin, and M.B. Hastings, Phys. Rev. Lett. **92**, 018303 (2004).
- <sup>18</sup> A. Hopkins, K. Jacobs, S. Habib and K. Schwab, Phys. Rev. B **68**, 235328 (2003).
- <sup>19</sup> Ya. M. Blanter and M. Büttiker, Phys. Rep. **336**, 1 (2000).
- <sup>20</sup> D.K. Ferry and S.M. Goodnick, *Transport in Nanostructures*, (Cambridge University Press, Cambridge, UK, 1997).
- <sup>21</sup> U. Hanke, Yu. Galperin, K.A. Chao, M. Gisselält, M. Jonson and R.I. Shekter, Phys. Rev. B **51**, 9084 (1995).
- <sup>22</sup> H.B. Sun and G.J. Milburn, Phys. Rev. B **59**, 10748 (1999).
- <sup>23</sup> A.N. Korotkov, Phys. Rev. B **49**, 10381 (1994).
- <sup>24</sup> This is consistent with previous treatments of the SET which usually make the assumption that when  $C_g \ll C_j$ , one can set  $a = b = 1/2$ , as discussed in Ref. 21.
- <sup>25</sup> R. Aguado and T. Brandes, Phys. Rev. Lett. **92**, 206601 (2004).
- <sup>26</sup> D.K.C. MacDonald, *Noise and Fluctuations: an Introduction*, (John Wiley, NY, 1962).
- <sup>27</sup> D.K.C. MacDonald, Phil. Mag. **40**, 561 (1949).
- <sup>28</sup> R. Ruskov and A.N. Korotkov, Phys. Rev. B **67**, 075303 (2003).
- <sup>29</sup> D. Mozyrsky, L. Fedichkin, S.A. Gurvitz and G.P. Berman, Phys. Rev. B **66**, R161313 (2002).
- <sup>30</sup> W.H. Press, S.A. Teukolsky, W.T. Vetterling, and B.P. Flannery, *Numerical Recipes in Fortran*, 2nd ed. (Cambridge University Press, Cambridge, UK, 1992).
- <sup>31</sup> The range of values of  $\epsilon$  and  $\kappa$  which might be achieved in practice is discussed in Ref. 14, but in general it is expected that SET-resonator systems will operate in the regime where  $\epsilon, \kappa \ll 1$ .
- <sup>32</sup> E.V. Sukhorukov, G. Burkard and D. Loss, Phys. Rev. B **63**, 125315 (2001).
- <sup>33</sup> C.W. Gardiner, *Handbook of Stochastic Methods for Physics, Chemistry and the Natural Sciences*, (2nd ed. Springer-Verlag, Berlin, Germany 1985).
- <sup>34</sup> This is readily found from the approximate solution for the charge-charge correlation function, valid for  $\epsilon \ll 1$ , that is obtained via the approach used to solve the mean coordinate equations in Ref. 14.
- <sup>35</sup> F. Pistolesi, Phys. Rev. B **69**, 245409 (2004).
- <sup>36</sup> A. Isacson and T. Nord, Europhys. Lett. **66**, 708 (2004).
- <sup>37</sup> T. Novotný, A. Donarini, C. Flindt and A.-P. Jauho, Phys. Rev. Lett. **92**, 248302 (2004).